

# Biotic and Abiotic Controls Over Canopy Function and Structure in Humid Hawaiian Forests

Christopher S. Balzotti\* and Gregory P. Asner

*Department of Global Ecology, Carnegie Institution for Science, 206 Panama Street, Stanford, California 94305, USA*

## ABSTRACT

Foliar nitrogen (N) plays a key role in ecosystem function and dynamics, including processes such as photosynthesis, productivity, and decomposition. Aboveground carbon density (ACD  $\text{Mg C ha}^{-1}$ ) represents a cumulative functional outcome of these and other ecosystem processes and is an important metric for monitoring current carbon stocks. Despite their importance, multiple interacting controls over landscape-level variation in foliar N and ACD are poorly understood. We assessed the relative importance of individual ecologically important state factors (climate, substrate, age, vegetation, and topography) associated with canopy foliar N and ACD throughout a humid forest landscape. We combined high-resolution remotely sensed data, machine learning, and field data to map and assess canopy foliar N and ACD patterns across a 5016-ha forest reserve in Hawai'i. Distance to non-native forests had the largest relative influence on canopy foliar N concentration,

followed by mean annual temperature (MAT), vegetation type, precipitation, soil, canopy height, and substrate age. In contrast, soil type was the strongest determinant of spatial variability in ACD, followed by precipitation, MAT, and vegetation type. Similar to foliar N, climate and vegetation variables were associated with ACD. However, soil type was found to be much more important in the ACD model (30%) than in the foliar N model (4%). Landscape-scale patterns in canopy foliar N and ACD are the result of shifts in vegetation type and composition, most likely due to species' responses to past disturbances, current climate conditions, and available nutrients. Degradation of native forests and future climate changes could result in highly altered biogeochemical cycles.

**Key words:** carbon storage; Carnegie Airborne Observatory; foliar nitrogen; gradient boosting; LiDAR.

## INTRODUCTION

Forests cover roughly 30% of the global land surface and provide numerous ecological, biogeochemical, economic, and cultural services (Bonan

2008). Multiple factors, such as climate, geologic substrate, and human activities, strongly influence forest structure and function, and thus the services provided by forests (for example, Jenny 1941; Amundson and Jenny 1991; Vitousek 2004; Morris 2010), but our knowledge of these controls has been mostly gleaned from univariate environmental gradients that isolate individual factors affecting forests (Pickett 1989; Vitousek 2004) or climate-centric work done at coarse spatial scales, that is, map units greater than 30 m (for example, Woodward and others 1995; Liu and others 2014).

Received 31 October 2016; accepted 9 April 2017;  
published online 28 April 2017

**Author Contributions** CSB and GPA conceived of or designed study, performed research, analyzed data, contributed new methods or models, and wrote the paper.

\*Corresponding author; e-mail: cbalzotti@carnegiescience.edu

In comparison, little is known about the relative influence of abiotic and biotic factors combined, and their interactions, on forest structure and functioning at finer spatial scales (or grain sizes) across large heterogeneous landscapes (Ollinger and others 2002; Asner and others 2009; McNeil and others 2012).

Two common metrics utilized in past studies to assess forest function are foliar nitrogen (N) concentration (for example, McNeil and others 2008; Chen and others 2013) and aboveground carbon density (ACD  $\text{Mg C ha}^{-1}$ ; Zolkos and others 2013). Foliar N concentration plays a central role in ecosystem function and dynamics and is linked to important processes, including maximum photosynthetic capacity, productivity, and litter decomposition (Field 1983; Field and Mooney 1983). Canopy foliar N concentration generally reflects soil N availability and is considered an indicator of forest ecosystem N cycling (Vitousek 2004; McNeil and others 2008). Aboveground carbon density, on the other hand, represents the cumulative functional outcome of these and other processes and is an important metric for monitoring current carbon stocks and understanding the global carbon cycle. Despite their importance and recent work (see below), controls over landscape-level variation in foliar N and ACD are still not fully understood (Asner and others 2009).

Recent advances that combine remote sensing technology with field data have made high-resolution mapping (map unit  $\leq 30$  m) of ACD and canopy nutrients a possibility, allowing researchers the ability to quantitatively assess continuous ACD and canopy nutrient data over large heterogeneous landscapes. At the forefront of this work is the use of light detection and ranging (LiDAR) for ACD, and imaging spectroscopy for canopy nutrients. LiDAR has been used to create accurate high-resolution ACD maps of forests across the globe (Zolkos and others 2013), including our study region (Asner and others 2016). Similarly, imaging spectroscopy has recently been used to create high-resolution maps of canopy foliar N in temperate (for example, Ollinger and others 2002; Lepine and others 2016) and tropical forests (for example, Asner and others 2015b; Chadwick and Asner 2016).

Relating spatial patterns of canopy foliar N and ACD to underlying environmental gradients can be used to reveal key factors regulating ecosystem processes (McNeil and others 2012). Factors shown to correlate with canopy foliar N and ACD in forest ecosystems across multiple spatial scales and forest types include climate (for example, Craine and others 2009; Liu and others 2014), vegetation type

(for example, Fyllas and others 2009; McNeil and others 2012), topography (for example, de Castilho and others 2006; Detto and others 2013), human disturbance (for example, Ollinger and others 2002; McNeil and others 2012), soils (Quesada and others 2012), and time, that is, substrate age (Vitousek and Farrington 1997; Vitousek 2004).

Forest canopy foliar N typically increases with increasing mean annual temperature (MAT) and decreasing mean annual precipitation (MAP; Schuur and Matson 2001; Craine and others 2009). Similar to canopy foliar N, global mature forest ACD increases with increasing MAT, but has an opposite response to MAP (Liu and others 2014). However, tropical forest ACD shows a similar trend to canopy foliar N, with ACD increasing with increasing MAT and decreasing MAP (Schuur and Matson 2001; Liu and others 2014). In addition to climate, forest composition can strongly influence canopy foliar N and ACD patterns through the collective investment strategies and physiological adaptations of the individual trees in response to their environment (Rien and Chapin 2000; McNeil and others 2008; Asner and others 2014). Likewise, topographic variability and slope position have been shown to strongly influence spatial patterns of ACD and foliar nutrients by creating heterogeneity in the hydrological network, intensity of natural and anthropogenic disturbances, solar radiation exposure, and nutrient availability (Luizão and others 2004; Detto and others 2013; Houlton and Morford 2015). Yet in other cases, topographic variables seem to play a lesser role in predicting ACD or canopy foliar N (McNeil and others 2012). Human disturbances, such as past forest clearing, can result in loss of available N that can translate to forests with lower canopy foliar N even decades after the disturbance (Vitousek and Jerry 1979; Ollinger and others 2002). However, if non-native species with adaptations (such as nitrogen fixing capabilities) invade the disturbance space, the resulting forest canopy can be higher in foliar N than the previous native forest (for example, Hughes and Denslow 2005). Soil composition also influences many aspects of nutrient cycling and plant growth such as water-holding capacity, soil temperature, and nutrient availability (Brady and Weil 2000). Furthermore, over geologic time scales, rock-derived nutrients important for ACD, such as phosphorous (P), decrease due to leaching, and N increases due to accumulation (Vitousek 2004; Porder 2015). This pattern can lead to higher canopy foliar N and greater ACD at mid-aged sites (Vitousek and others 1995). Identifying relationships between the factors that control nutrient cy-

cling and biomass accumulation in current tropical forests is critical for understanding how they will respond to future natural and human-driven environmental change (Cleveland and others 2011; McNeil and others 2012).

For decades, the Hawaiian islands have been used as a model system for understanding how ecosystems function (Townsend and others 1995; Vitousek 2004; Asner and others 2005; Kellner and Asner 2009). Hawai'i's native forests are also home to hundreds of endemic and endangered species that are deeply tied to Hawaiian cultural identity and sense of place (Sakai and others 2002; Ticktin and others 2006). Following European contact, native Hawaiian forests have rapidly changed from ecosystems comprised of an endemic flora to forests composed of recently introduced and expanding invasive species. Such changes in canopy composition can have profound effects on forest structure and functioning (Asner and others 2008; Vilà and others 2011).

The rapidly changing forests of Hawai'i provide an opportunity to evaluate the relative influence of biotic and abiotic factors that determine humid forest structure and function. Our objective was to assess the relative importance of individual state factors (climate, substrate, age, vegetation type and species, and topography) affecting forest canopy foliar N (% concentration, hereafter referred to as foliar N) and ACD. This was accomplished using a top-down approach that incorporates high-resolution remotely sensed data, computational machine learning, and field data, to map and assess foliar N and ACD patterns across a 5016-ha forest reserve. We know, from prior single-species studies in Hawai'i, that the dominant keystone forest canopy species 'ōhi'a (*Metrosideros polymorpha* Gaudich) shows a decrease in foliar N with decreasing temperature or increasing rainfall (Vitousek and others 1990, 1992; Schuur and Matson 2001). We also know from other tropical forests that foliar N is strongly mediated by phylogeny (Fyllas and others 2009; Asner and others 2014; Balzotti and others 2016). What is poorly known in humid forests of Hawai'i and elsewhere is the combined influence of all canopy species, in conjunction with other state factors, in spatially determining canopy foliar N concentrations and ACD.

## MATERIALS AND METHODS

### Study Region

The study region is located on the eastern slope of Mauna Kea volcano (Figure 1; 19°54'56.85"N,

155°17'23.02"W) and is part of the largest remaining native-dominated humid forest in Hawai'i (DLNR and USDA 2016). We evaluated foliar N and ACD in the Laupāhoehoe and Hilo Forest Reserves (hereafter referred to as Laupāhoehoe). These adjoining reserves cover about 5016 ha of tropical forest and are designated as part of the Hawai'i Experimental Tropical Forest (Asner and others 2009). Laupāhoehoe is an important watershed that provides habitat for numerous endemic and endangered flora and fauna, including 16 endangered plant taxa and Hawai'i's only native land mammal, the 'ōpe'ape'a (Hawaiian hoary bat; *Lasiurus semotus*; DLNR and USDA 2016). Laupāhoehoe was selected specifically for its cultural and environmental importance, extensive field data, geographic size, and variability among important ecological state factors. Laupāhoehoe ranges in elevation from 600 m to nearly 1900 m, resulting in a mean annual temperature (MAT) gradient from 18 to 13°C and a mean annual precipitation gradient (MAP) from about 1500 to 5000 mm. Although the common native canopy species, 'ōhi'a and koa (*Acacia koa* A. Gray), are found throughout Laupāhoehoe, forest canopy composition varies across the reserve (Asner and others 2009; Table 1). Ecosystems within Laupāhoehoe range from low-elevation wet tropical to mesic montane forests (Figure 2; Gon and others 2006). Invasive species are present throughout the reserve; however, prior studies (Asner and others 2009; Broadbent and others 2014; DLNR and USDA 2016) have identified and mapped very high concentrations of non-natives below about 1000 m (for example, *Psidium cattleianum* Sabine and *Ficus rubiginosa* Desf. Ex Vent.) and above about 1300 m (for example, *Fraxinus uhdei* (Wenzig) Lingelsh.; Asner and others 2009; Broadbent and others 2014; DLNR and USDA 2016). The mid-elevation forest, found between 1000 and 1300 m, is primarily closed 'ōhi'a and koa forest, with little impact from past human use or invasive species. The landscape above the reserve has been impacted by past grazing and is dominated by non-native grasses. The landscape below the reserve is made up of agricultural lands and plantation forests.

### Statistical Analysis

We used a gradient boosting machine model (Friedman 2001) to determine the relative influence of environmental and biotic factors on foliar N and ACD distribution patterns across Laupāhoehoe. Gradient boosting was chosen here for its ability to accommodate nonlinear interactions, resilience to

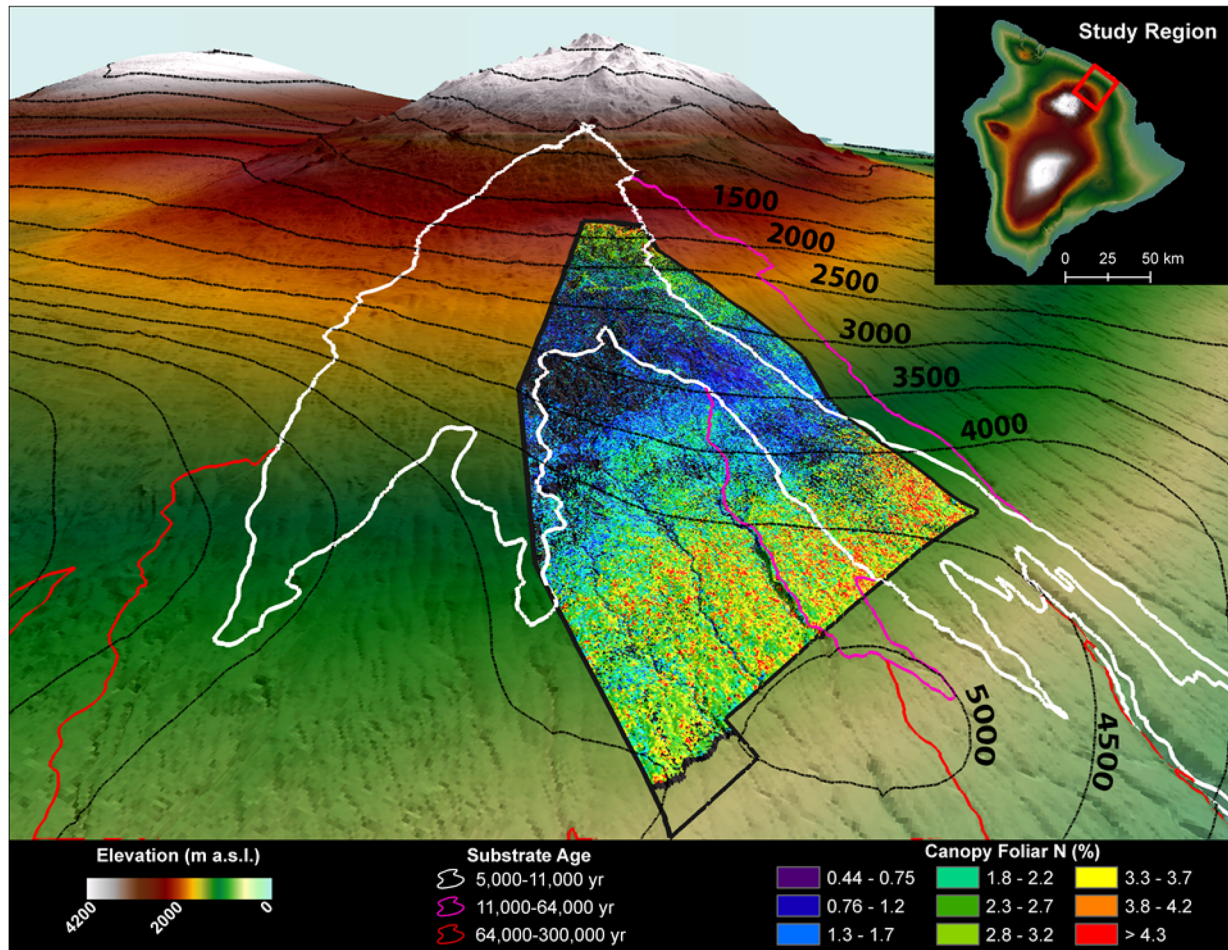


Figure 1. The study region located on the eastern slope Mauna Kea volcano, Hawai'i. Past lava flows are outlined in *white* (5000–11,000 years), *pink* (11,000–64,000 years) and *red* (64,000–300,000 years). The Carnegie Airborne Observatory-derived canopy foliar nitrogen (%) is shown with the highest values in *red* and the lowest in *dark purple*. The *dashed lines* with values are mean annual rainfall isohyets in mm (Color figure online).

outlier influence, tolerance of collinear predictor variables, and ability to handle categorical and missing data (Moisen and others 2006; Elith and others 2008). A detailed description of GBMs can be found in Hastie and others (2009) and Elith and others (2008). In short, GBMs are a decision tree-based regression technique that sequentially decreases model bias. Unlike other tree-based models, such as Random Forest, GBMs are computationally more intensive and require proper selection of metaparameters to prevent overfitting (Hastie and others 2009). We followed guidelines, provided by Elith and others (2008) and the R package *dismo* (Hijmans and others 2016), to choose model tuning parameters during the implementation of the GBM models. The final tuning parameters for the foliar N and ACD models included the number of decision trees, tree complexity (number of nodes), contribution of each tree to the growing model (learning

rate), and the loss function (Table 2). Model performance was evaluated by using a tenfold cross-validation calculation. Overall influence of each independent variable was evaluated by its relative influence on the model output. Relative influence was determined by how well each variable improves the model, averaged across all trees (Friedman and Meulman 2003). Additionally, the effect of each independent variable on the dependent variable was evaluated with partial dependency analysis, which plots the effect of each independent variable on the dependent variable, after accounting for the average effect of the other independent variables in the model (Hastie and others 2009).

We also evaluated changes in foliar N and ACD with changes in elevation alone, to determine whether there were distinct shifts in variance with elevation, between the previously identified closed canopy native forests and the highly invaded for-

**Table 1.** Percent Cover of Each Vegetation Type by Elevation in Laupāhoehoe and Hilo Forest Reserves

Vegetation type	Elevation (m a.s.l.)										
	700	800	900	1000	1100	1200	1300	1400	1500	1600	1700
Closed ohia wet forest	–	–	–	1.4	33.4	55.6	27.0	6.2	3.6	–	–
Closed koa ohia wet forest	14.0	61.4	99.8	95.3	52.1	34.8	68.5	79.4	56.8	16.0	–
Open ohia wet forest	–	–	–	3.3	14.4	9.4	0.9	1.5	0.5	–	–
Open koa ohia wet forest	0.4	0.1	–	–	–	–	–	–	2.6	0.2	–
Closed ohia mesic forest	–	–	–	–	–	–	–	–	0.1	–	–
Closed koa ohia mesic forest	–	–	–	–	–	–	–	–	1.8	53.4	42.5
Open ohia mesic forest	–	–	–	–	–	–	–	–	0.1	0.7	–
Open koa ohia mesic forest	–	–	–	–	–	–	–	–	–	24.0	49.2
Open koa mamane dry forest	–	–	–	–	–	–	–	–	–	–	0.2
Alien wet forest	–	–	–	–	<b>0.1</b>	–	<b>0.1</b>	<b>2.5</b>	<b>5.7</b>	<b>0.5</b>	–
Alien mesic forest	–	–	–	–	–	–	–	–	<b>0.5</b>	–	<b>0.7</b>
Plantation forest	–	–	–	–	–	–	–	<b>4.1</b>	<b>26.0</b>	<b>2.4</b>	<b>2.2</b>
Uluhe ferns and native shrubs	–	–	–	–	–	–	–	0.1	0.6	2.6	5.1
Alien wet grassland	–	–	–	–	–	0.1	–	–	1.3	–	–
Alien mesic grassland	–	–	–	–	–	–	–	–	–	0.3	–
Cultivated agriculture	–	–	–	–	–	–	–	–	–	–	–
Very sparse vegetation	–	–	–	–	–	–	–	0.1	0.2	–	–
Closed koa wet forest	–	–	–	–	–	–	3.5	6.0	–	–	–
Strawberry guava ficus invaded	<b>85.6</b>	<b>38.5</b>	<b>0.2</b>	–	–	–	–	–	–	–	–

*Vegetation types in bold are dominated by invasive or plantation tree species.*

ests, found at below 1000 m and above 1300 m (see above). Because variance in foliar N and ACD was heterogeneous between elevations, comparisons were made using Kruskal–Wallis nonparametric analysis of variance. When the Kruskal–Wallis analysis was significant ( $p < 0.05$ ), a Dunn’s post hoc test was performed to identify which elevations differed statistically from each other. All statistical analyses were performed in R 3.2.4 (R Development Core Team 2016).

### Carnegie Airborne Observatory Data

In January 2016, the Carnegie Airborne Observatory (CAO) deployed its most advanced remote sensing platform to date in Hawai’i, the third-generation Airborne Taxonomic Mapping System (AToMS; <https://cao.carnegiescience.edu/>; Asner and others 2012). CAO-AToMS was equipped with three remote sensing technologies integrated to produce high-dimensional orthorectified data. CAO-AToMS contained a high-fidelity visible-shortwave infrared imaging spectrometer (HiFIS), dual-laser waveform light detection and ranging (LiDAR) scanner, and a visible-to-near infrared (VNIR) imaging spectrometer. The data were collected using the CAO Dornier 228 aircraft, from an altitude of 2000 m above ground level (a.g.l.), at an

average ground speed of 241 km h<sup>-1</sup>, resulting in a mapping swath of roughly 1200 m. For this study, we used data from the LiDAR and the HiFIS sensors to generate high-resolution digital terrain models (DTM), top-of-canopy height models (TCH), and canopy reflectance models. The DTM, TCH, and reflectance models were then used to create additional geomorphometric, ACD, and foliar N maps (see below; Figure 3).

The settings used for the LiDAR were 34° field of view, a pulse frequency of 100 kHz per laser, and a beam divergence of 0.56 mrad (1/e) per laser, allowing for a minimum of four laser shots per m<sup>2</sup>. The LiDAR data were combined with embedded global positioning system–inertial measurement unit (GPS-IMU) data, and a smoothed best estimate of trajectory (SBET) was computed to determine the 3-D locations of each laser return, producing a LiDAR data “point cloud.” The resulting points were then interpolated into a raster DTM at a mapping resolution of 1.0 m. Ground returns were classified using the lasground program, which is part of the LAsTools suite (Rapidlasso, GmbH; Gilching, Germany). We used the options “extra fine” and “offset 1.” The DTM model was interpolated from a triangular irregular network (TIN) model, created from the ground points, and the TCH was interpolated from a TIN model, fit to first

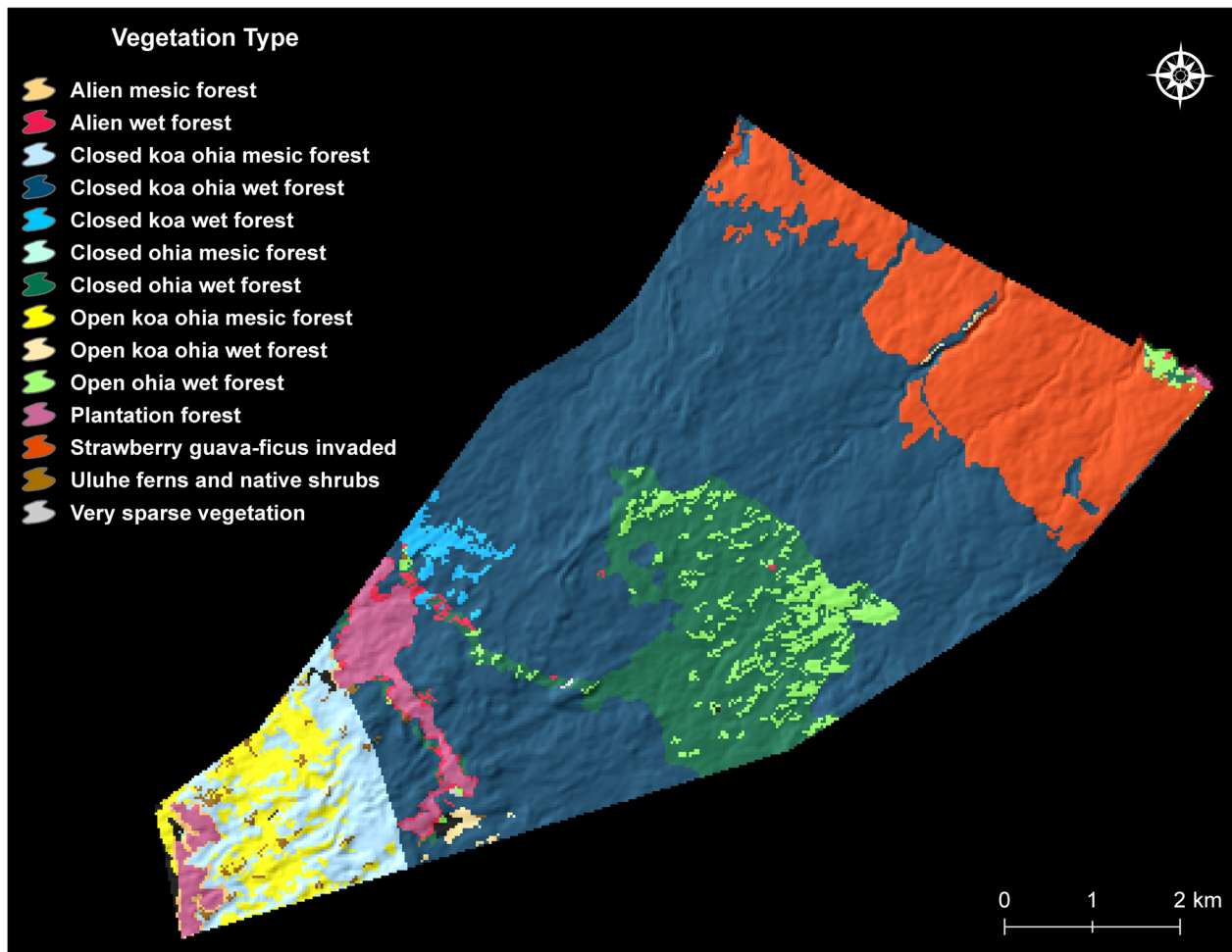


Figure 2. Vegetation cover type determined using the Hawai'i Gap Analysis Program (GAP) map (Gon and others 2006), updated with an additional invasive species class determined by Asner and others (2009) (Color figure online)

**Table 2.** Metaparameters Used for the Gradient Boosting Models (GBM) for Canopy Foliar N (% Concentration) and Aboveground Carbon Density (ACD Mg C ha<sup>-1</sup>)

Metaparameters	Canopy foliar N (%)	Aboveground carbon density (ACD)
Number of decision trees	2550	4000
Tree complexity	8	3
Learning rate	0.005	0.005
Loss function	Laplace	Laplace

returns, adjusted for height above the ground TIN model. Validation studies of the CAO-derived TCH, across a wide range of studies, including Hawai'i, have shown this approach to be highly accurate (Asner and others 2016). ACD was determined at a mapping resolution of 30 m, using the TCH and the CAO Hawai'i allometric ACD calibration equation:  $ACD = 3.744 \times TCH^{1.391}$  (Asner and others 2016). The final digital terrain data were coarsened to a spatial resolution of 30 m and were used to gen-

erate eleven common geomorphometric models representing topography throughout the study region (Table 3).

The HiFIS imaging spectrometer measures spectral radiance in 427 channels (bands), spanning the 380–2510 nm wavelength range in 5 nm increments with nominal 6 nm spectral response function (full width at half maximum). The HiFIS data went through extensive preprocessing in preparation for mapping foliar N (Figure 3; Asner and

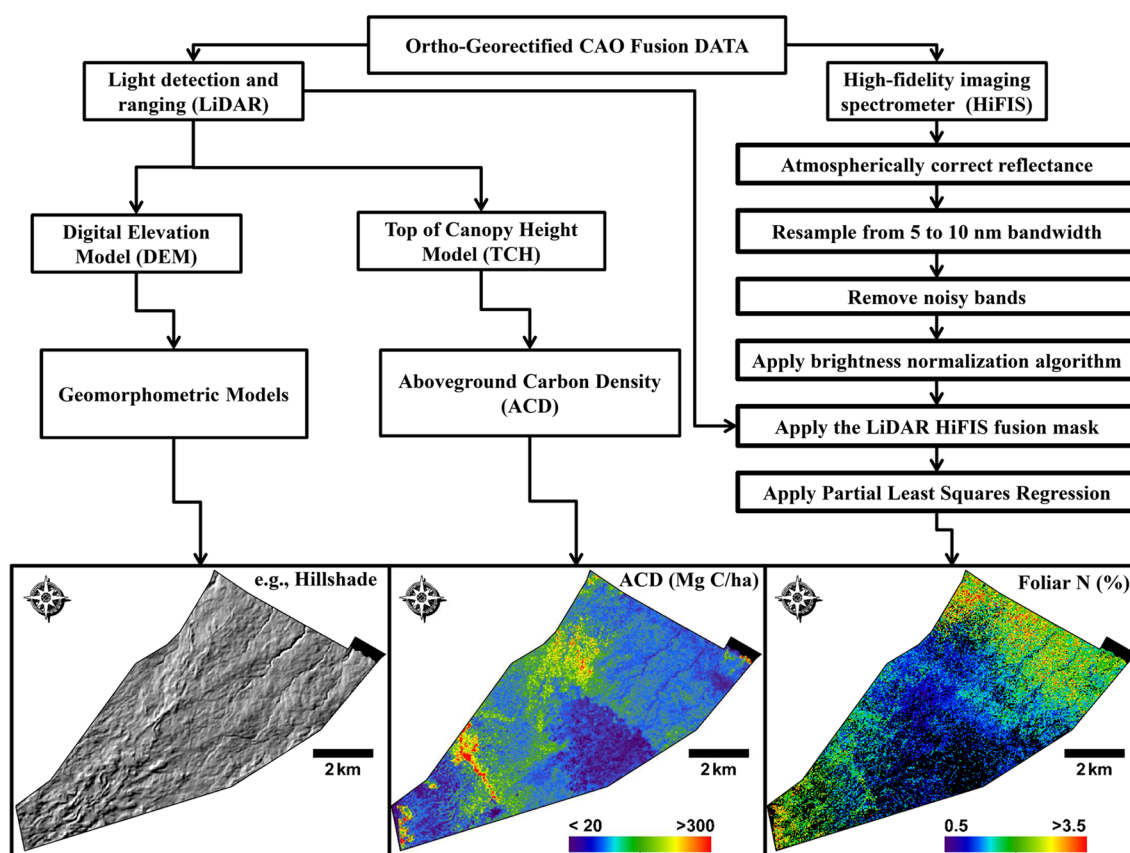


Figure 3. General workflow for producing aboveground carbon (ACD  $\text{Mg C ha}^{-1}$ ) density and canopy foliar nitrogen (%) maps from the Carnegie Airborne Observatory light detection and ranging (LiDAR) and high-fidelity visible-shortwave infrared imaging spectrometer (HiFIS) data (Color figure online).

others 2015a). Prior to analysis, the 2.0-m spatial resolution HiFIS data were atmospherically corrected to surface reflectance using the ACORN-5 model (ImSpec LLC, Glendale, CA, USA), in an iterative mode with corrections for cross-track brightness variation (Colgan and others 2012). The ACORN model settings applied to the HiFIS data consisted of a model that provides a water vapor fit using wavelengths at 940 and 1130 nm, and aerosol settings by flight line determined in an iterative manner to ensure consistent scaling for vegetated pixels. No noise suppression was used, or ground targets for spectral smoothing. After atmospheric correction, bands in the range of atmospheric water absorption (1350–1480, 1780–2032 nm) and noisy bands in the far ends of the spectra (<410, >2450 nm) were removed. To reduce the influence of canopy leaf tissue orientation and depth, the reflectance data were brightness-normalized, following Feilhauer and others (2010). The brightness-normalized data were further filtered to remove bare ground, non-photosynthetic vegetation, clouds, and canopy shadow using a

LiDAR\HiFIS fusion mask (Asner and others 2007). In short, the LiDAR data were used to remove pixels with vegetation below 2 m and to create a ray-tracing model that incorporates solar viewing geometry to mask out canopy pixels that were in shade at the time of the flight. The HiFIS data were analyzed to mask out clouds and non-photosynthetic vegetation.

The prepared and filtered reflectance data were used to create a foliar N metric for the study region. Foliar N was determined using partial least squares regression (PLSR; Haaland and Thomas 1988). PLSR was chosen due to its extensive use in foliar N mapping across forest types and sensors (Ollinger and others 2002; Townsend and others 2003; Singh and others 2015). Similar to principal components analysis, PLSR converts the highly correlated spectral bands to uncorrelated variables (latent vectors). These latent vectors are created via an optimization process that involves dimensionality reduction and cross-validated linear regression (Feilhauer and others 2010). A tropical foliar N model was first built and validated using a network

**Table 3.** Topographic Variables Generated from the Carnegie Airborne Observatory (CAO) Light Detection and Ranging (LiDAR) Data

Variable	References	GIS software	Ecological and hydrological significance
Linear aspect	Stage (1976)	ArcGIS Geomorphometry and Gradient Metrics Tool-box 2.2 (Evans and others 2014)	Solar radiation and flow direction
Compound Topographic Index (CTI)	Moore and others (1993) and Gessler and others (1995)	ArcGIS Geomorphometry and Gradient Metrics Tool-box 2.2 (Evans and others 2014)	Soil moisture potential
Dissection	Evans (1972)	ArcGIS Geomorphometry and Gradient Metrics Tool-box 2.2 (Evans and others 2014)	Heterogeneity of the landscape
Heat Load Index (HLI)	McCune and Keon (2002)	ArcGIS Geomorphometry and Gradient Metrics Tool-box 2.2 (Evans and others 2014)	Local temperature and moisture
Planar curvature	Zevenbergen and Thorne (1987)	ESRI 2011. ArcGIS Desktop: Release 10.2. Redlands, CA: Environmental Systems Research Institute	Convergence/divergence of flow
Profile curvature	Zevenbergen and Thorne (1987)	ESRI 2011. ArcGIS Desktop: Release 10.2. Redlands, CA: Environmental Systems Research Institute	Rate of flow (erosion/deposition) across the surface
Site Exposure Index (SEI)	Ballice and others (2000)	ArcGIS Geomorphometry and Gradient Metrics Tool-box 2.2 (Evans and others 2014)	Solar radiation and wind exposure
Slope	Horn (1981)	ESRI 2011. ArcGIS Desktop: Release 10.2. Redlands, CA: Environmental Systems Research Institute	Hydrological flow and site stability
Surface relief ratio	Pike and Wilson (1971)	ArcGIS Geomorphometry and Gradient Metrics Tool-box 2.2 (Evans and others 2014)	Heterogeneity of the landscape
Total curvature	Zevenbergen and Thorne (1987)	ESRI 2011. ArcGIS Desktop: Release 10.2. Redlands, CA: Environmental Systems Research Institute	Concavity and convexity
Vector ruggedness model (VRM)	Sappington and others (2007)	Benthic Terrain Modeler tool for ArcGIS 3.0 (Wright and others 2012)	Terrain complexity incorporating slope and aspect gradient variability

of 79 field plots, located in 22 tropical forest types across a 3500-m elevation gradient in Peru (Asner and others 2014). The tropical foliar N model was successfully tested in Costa Rica with similar results as Peru ( $R^2 = 0.28\text{--}0.59$ , RMSE = 0.07–0.11) (Bazzotti and others 2016), before it was applied to Laupāhoehoe.

### Additional Input Data

Six additional independent variables were used in the modeling of foliar N and ACD distributions (Table 4): MAT, MAP, substrate age, soil type, vegetation type, and distance to non-native forests. MAT data were obtained from the Climate of Hawai'i Web site, University of Hawai'i at Mānoa (<http://climate.geography.hawaii.edu/>; Giambelluca and others 2014). MAP data were obtained from the Rainfall Atlas of Hawai'i (<http://rainfall.geography.hawaii.edu/>; Giambelluca and others 2013). Substrate age was determined using the geologic map of Hawai'i, produced by Sherrod and others (2007), and obtained from <http://pubs.usgs.gov/of/2007/1089/>. Soil classification maps were obtained from the Soil Survey Geographic (SSURGO 2015) database <http://websoilsurvey.nrcs.usda.gov>. Vegetation cover type was determined using the Hawai'i Gap Analysis Program (GAP) map (Gon and others 2006), updated by Jacobi and others (Selmants and others 2017) with an additional invasive species class determined by Asner and others (2009; Figure 2). Disturbances in the Laupāhoehoe reserve are decades old with the plantations and invaded forests in a mature state (Asner and others 2009). To capture the potential influence of these past disturbances, the updated GAP vegetation map was used, and the Euclidian distance to non-native and plantation forests was determined with ArcGIS® software (Release 10.2 Redlands, CA: Environmental Systems Research Institute).

### RESULTS

The GBM model performed well in determining both foliar N and ACD. The foliar N model tenfold cross-validation reported a mean  $R^2$  of  $0.76 \pm 0.002$  (SE) and a RMSE of 0.40%. The ACD model performed slightly better, with a mean cross-validation  $R^2$  of  $0.77 \pm 0.003$  and a RMSE of  $37.8 \text{ Mg C ha}^{-1}$ . For the foliar N model, distance to non-native forests had the largest relative influence (60%) of all the factors included, followed by MAT (12%), vegetation type (8%), MAP (5%), soil type

**Table 4.** Independent Variables Used in the Gradient Boosting Model

Variables	Name in model
Climate	–
Mean annual precipitation	MAP
Mean annual temperature	MAT
Topography	–
Aspect	Aspect
Compound Topographic Index	CTI
Dissection	Dissection
Heat Load Index	HLI
Planar curvature	Planar curve
Profile curvature	Profile curve
Site Exposure Index	SEI
Slope	Slope
Surface relief ratio	SRR
Total curvature	Total curve
Vector ruggedness model	VRM
Vegetation	–
Closed ohia wet forest	1
Closed koa ohia wet forest	2
Open ohia wet forest	4
Open koa ohia wet forest	5
Closed ohia mesic forest	6
Closed koa ohia mesic forest	8
Open koa ohia mesic forest	10
Alien wet forest	19
Alien mesic forest	20
Plantation forest	23
Uluhe ferns and native shrubs	30
Closed koa wet forest	101
Strawberry guava ficus invaded forest	102
CAO-derived top-of-canopy height	TCH
Substrate age	–
5000–11,000 years	6
13,000–30,000 years	7
64,000–300,000 years	9
Soils name (SSURGO)	–
Akaka–Onomea complex, 0–10% slopes	72
Maile-Waiakea-Rock outcrop complex, 6–35% slopes	140
Honokaa highly organic hydrous silty clay loam, 10–20% slopes	143
Kau very cobbly highly organic medial loam, 6–20% slopes	320
Kaiwiki highly organic hydrous silty clay loam, 6–20% slopes	385
Waiakea very cobbly hydrous loam, 10–20% slopes	478

(4%), TCH (3%), and substrate age (1%). None of the topographic variables had a relative influence greater than 1% (Figure 4). These results suggest that disturbance, climate, and vegetation type (in-

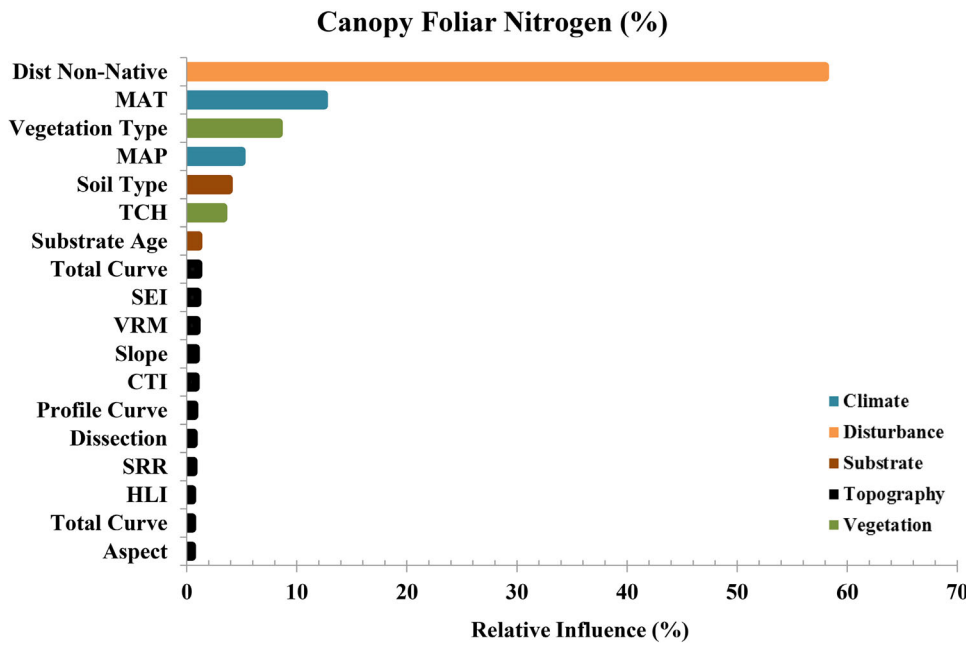


Figure 4. Relative influence plot generated from the gradient boosting machine (GBM) model for canopy foliar nitrogen (%) (Color figure online).

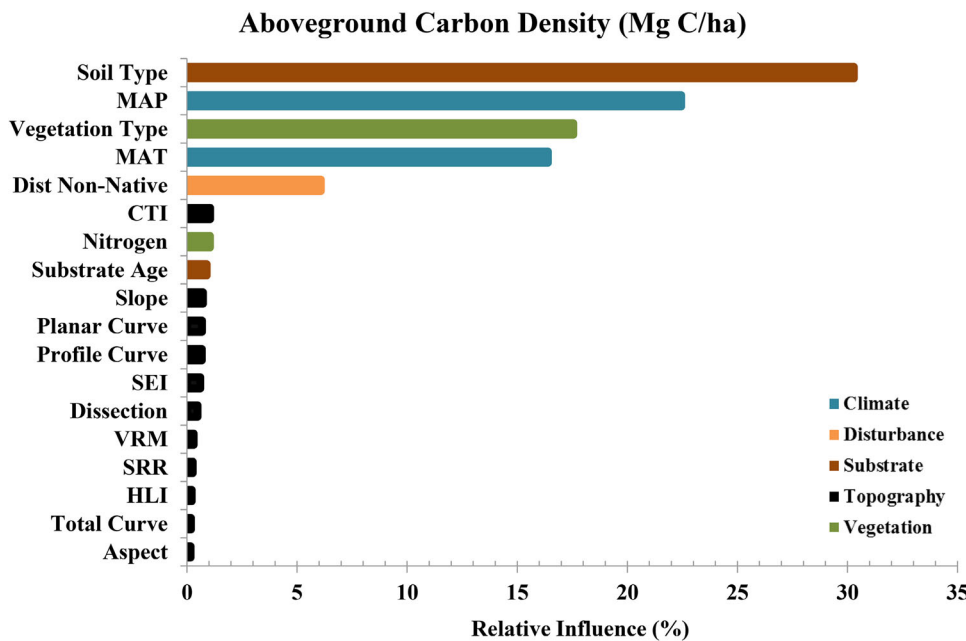


Figure 5. Relative influence plot generated from the gradient boosting machine (GBM) model for aboveground carbon density (ACD Mg C ha<sup>-1</sup>) (Color figure online).

cluding invasive species) are the most strongly interrelated factors influencing foliar N in humid Hawaiian forests.

For ACD, soil type was the most important factor (30%), followed by MAP (22%), vegetation type (18%), MAT (16%), and distance to non-native forests (6%). Substrate age, foliar N content, and the topographic variables had relative influence values no greater than 1% (Figure 5). Similar to foliar N, climate and vegetation type were associated with ACD. However, soil type was much more

important in the ACD model (31%) than the foliar N model (4%).

Partial dependency analyses (Figure 6) indicated that, in Laupāhoehoe, higher foliar N was found in areas closest to past disturbance with higher MAT and MAP between roughly 2000 and 2500 mm, in forests dominated by invasive species, shrublands, or open koa-‘ōhi’a mesic landscapes (Figure 2; Table 1). Additionally, partial dependency analyses revealed a sharp drop in foliar N at roughly 1000 m from non-native vegetation and a rapid increase in

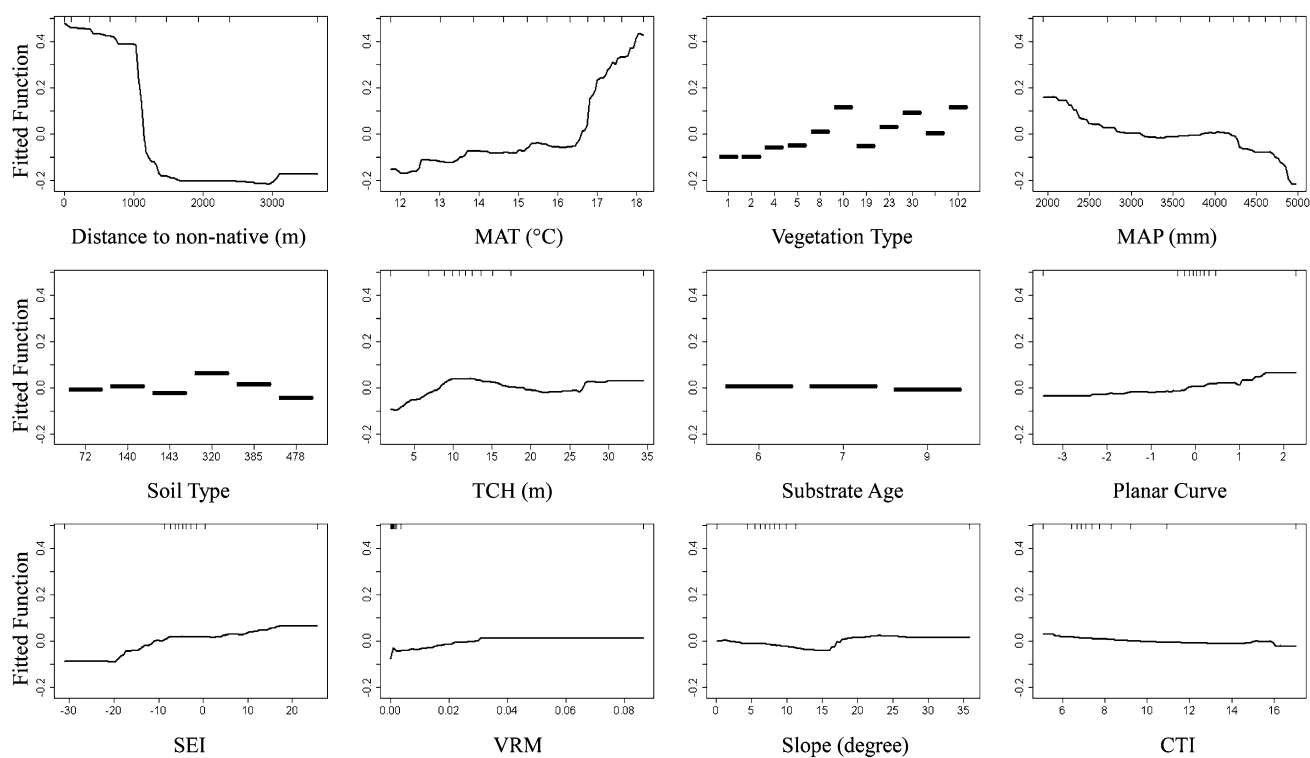


**Figure 6.** Partial dependency plots for the top 12 influential variables of the canopy foliar nitrogen (%) model. The Y-axis values represent the outcome of the model in relation to each independent variable, after accounting for the average effect of the other independent variables in the model. Rungs on the X-axis represent the spread of the data. Percentages given next to variable names are the relative influence values in the model. Full names for each of the variables are given in Table 4.

foliar N at temperatures above 16°C, suggesting potential distance to non-native vegetation and climatic thresholds for higher foliar N.

Partial dependency analyses for ACD indicated higher carbon stocks in forests on highly organic, hydrous silty clay loam and very cobbly hydrous loam soils, MAP between roughly 2000–4000 mm and higher MAT, in plantation or closed koa wet forests (Figure 7). The ACD partial dependency plot for MAT also showed an increase in ACD above temperatures of approximately 15°C.

There were distinct spatial patterns of foliar N and ACD along the elevation gradient in Laupāhoehoe (Figures 8 and 9) associated with the above-listed factors. Within the previously identified, mid-elevation, native-dominated portion of the landscape (1000–1300 m), foliar N decreased with elevation, following a similar pattern as earlier field studies (Vitousek and others 1990, 1992). At lower elevations dominated by invasive species, foliar N was significantly higher, with mean values nearly twice that of mid-elevation forests (Figure 8). For example, mean foliar N values were

2.2% at 700 m, compared to 1.3% at 1000 m. Additionally, ACD at lower elevations was significantly reduced (Figure 9), due to the shorter stature of the dominant invasive species (for example, strawberry guava).

Above 1400 m, mean foliar N showed a linear increase with increasing elevation. This increase in foliar N with higher elevation was an opposite trend from what was previously observed, when only ‘ōhi‘a was measured in native-dominated forests (Vitousek and others 1990, 1992) and instead coincided with an increase in invasive species and plantation forest cover, non-native vegetation (Table 1), canopy openness, and recent ‘ōhi‘a cohort dieback (Asner and others 2009). Furthermore, between 1500- and 1600-m elevation, a plantation forest of tropical ash [*F. uhdei* (Wenzig) Lingelsh.], planted in 1936, contained higher foliar N and ACD than the surrounding native koa- and ‘ōhi‘a-dominated forest. Finally, the highest elevation mesic forests had a similar mean foliar N (2.0%) and lower mean ACD than that of the lower elevation tropical wet forests.

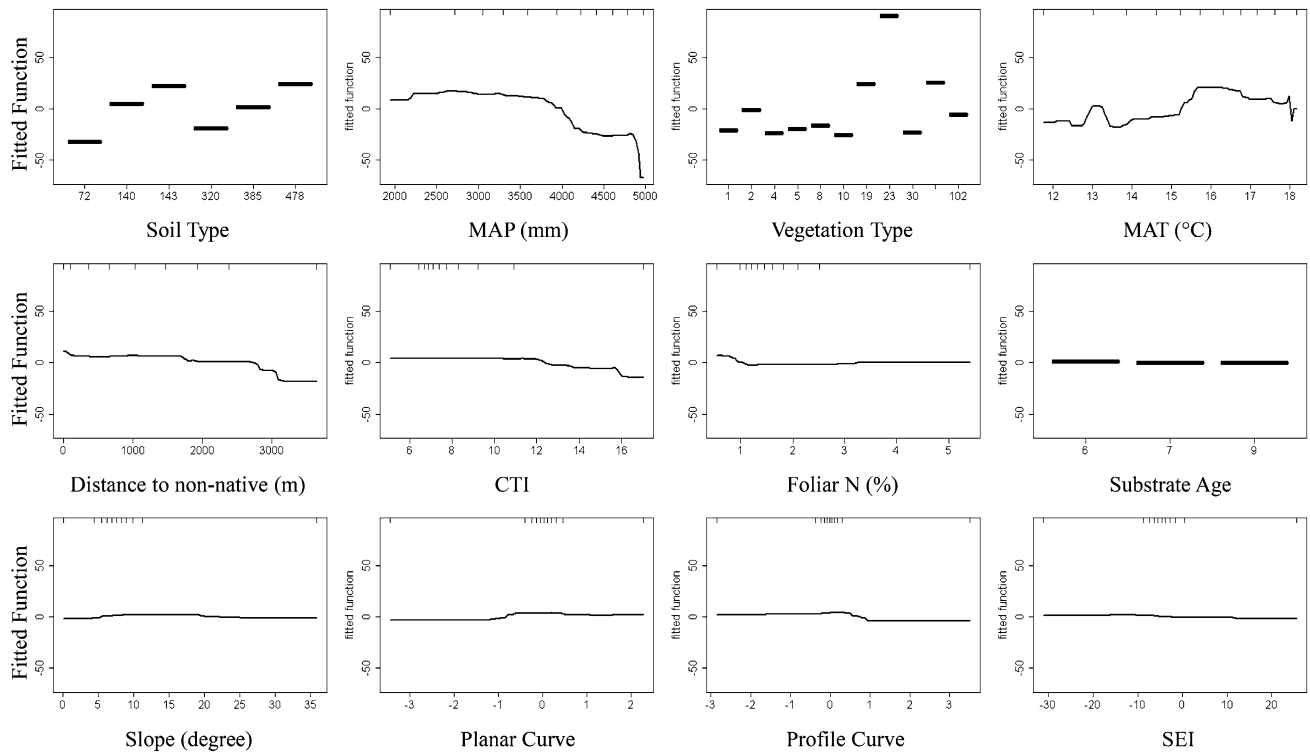


**Figure 7.** Partial dependency plots for the top 12 influential variables of the aboveground carbon density model. The Y-axis values represent the outcome of the model in relation to each independent variable, after accounting for the average effect of the other independent variables in the model. Rungs on the X-axis represent the spread of the data. Percentages given next to variable names are the relative influence values in the model. Full names for each of the variables are given in Table 4.

## DISCUSSION

By combining high-resolution remote sensing and a machine learning algorithm, we evaluated continuous patterns of forest foliar N and ACD across multiple ecological state factors and calculated the relative influence of each factor associated with foliar N and ACD. We found that, throughout the humid forests of Laupāhoehoe, distance from non-native forests, climate, and vegetation were the principal drivers of spatial variation in foliar N, whereas for ACD, soil, climate, and vegetation were the most influential predictors, highlighting stronger abiotic controls over ACD. What was surprising was how little the other factors influenced foliar N or ACD (Figures 3 and 4). Additionally, minimally invaded mid-elevation forests (1000–1300 m) differed substantially in structure and foliar N concentration from that of the surrounding forest, indicating a potential forest-wide shift in N cycling and structure with increasing invasion. This potential shift may be linked to physiological traits associated with invasive species, such as rapid growth rates, elevated leaf nutrient concentrations,

and high specific leaf area (Van Kleunen and others 2010), which improve litter quality and decomposition rates and which contribute to a positive feedback between invasive species and nitrogen cycling rates (Allison and Vitousek 2004; Hughes and Denslow 2005; Liao and others 2008). A meta-analysis of 94 experimental studies by Liao and others (2008) found that invaded ecosystems showed significant increases (50–150%) in flux variables, such as aboveground net primary production and litter decomposition, as well as a 40% increase in plant N concentration. A similar study to ours on foliar N in a temperate forest using multiple regression analysis found that species composition and disturbance were the strongest predictors of canopy foliar N compared to abiotic gradients of resource availability (McNeil and others 2012), suggesting a general pattern of influence.

Foliar N concentrations in Laupāhoehoe, and elsewhere, have been shown to reflect soil N availability (Vitousek 2004). The lower importance of soil type in the foliar N model, when compared to climate and vegetation, suggests that differences

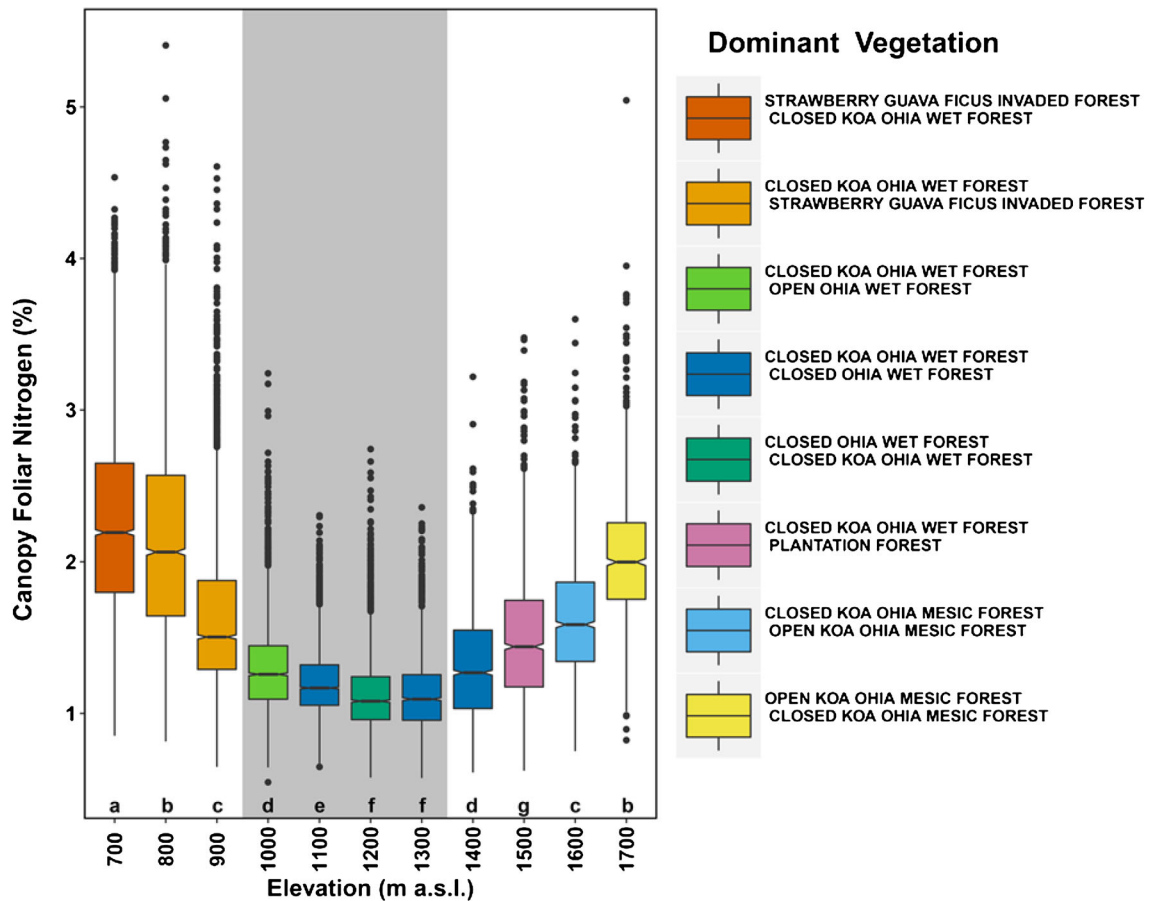


Figure 8. Canopy foliar nitrogen (%) by elevation. Elevations with *different lowercase letters* above the *X*-axis differ statistically ( $p < 0.05$ ). The boxplots are *color-coded* by the two most dominant forest types at each elevation; see Table 1 for percent cover for all forest types present at each elevation. The elevations between 1000 and 1300 m shown in *gray* are the least impacted by invasive species (Color figure online).

in N availability between the soil types were diminished by forest composition and climate interactions. In contrast, for ACD, some soils may reduce the simple effects of climate (for example, low temperatures, water saturation) on accumulated biomass. This has been observed in humid forests of the Amazon basin, where Levine and others (2016) found that water stress and spatial variation in soil texture explained aboveground biomass patterns. Additionally, Selmants and others (2014) found that, in the tallest native forests of Laupāhoehoe, MAT had almost no effect on aboveground carbon stocks. They suggested that variation in other factors, such as soil physical and chemical properties, was more closely tied to variability in tropical forest biomass. Furthermore, soils in Laupāhoehoe may be spatially organized by species composition, and therefore structure, at a finer grain than what was captured by the vegetation map used in our model. Further investigation

is needed into the capacity of soils to minimize the effects of climate on the biomass of these and other forests.

We know from prior studies in Hawai'i and elsewhere that substrate age and topography can be strong predictors of foliar nutrients and ACD (Vitousek 2004; Taylor and others 2015; Balzotti and others 2016). However, in our model, substrate age and topography had little influence on foliar N or ACD. The relatively weak influence of substrate age, at Laupāhoehoe, may be due to the age classes present throughout the reserve (~5–300 ky). All of these classes would be considered “mid-aged” when compared to the well-studied long substrate age gradient (0.3–4100 ky) across the Hawaiian archipelago (Vitousek 2004). Mid-aged substrates in Hawai'i are relatively rich in available soil N and phosphorous, potentially minimizing the local-scale influence of substrate age, after accounting for the average effects of the other variables in the

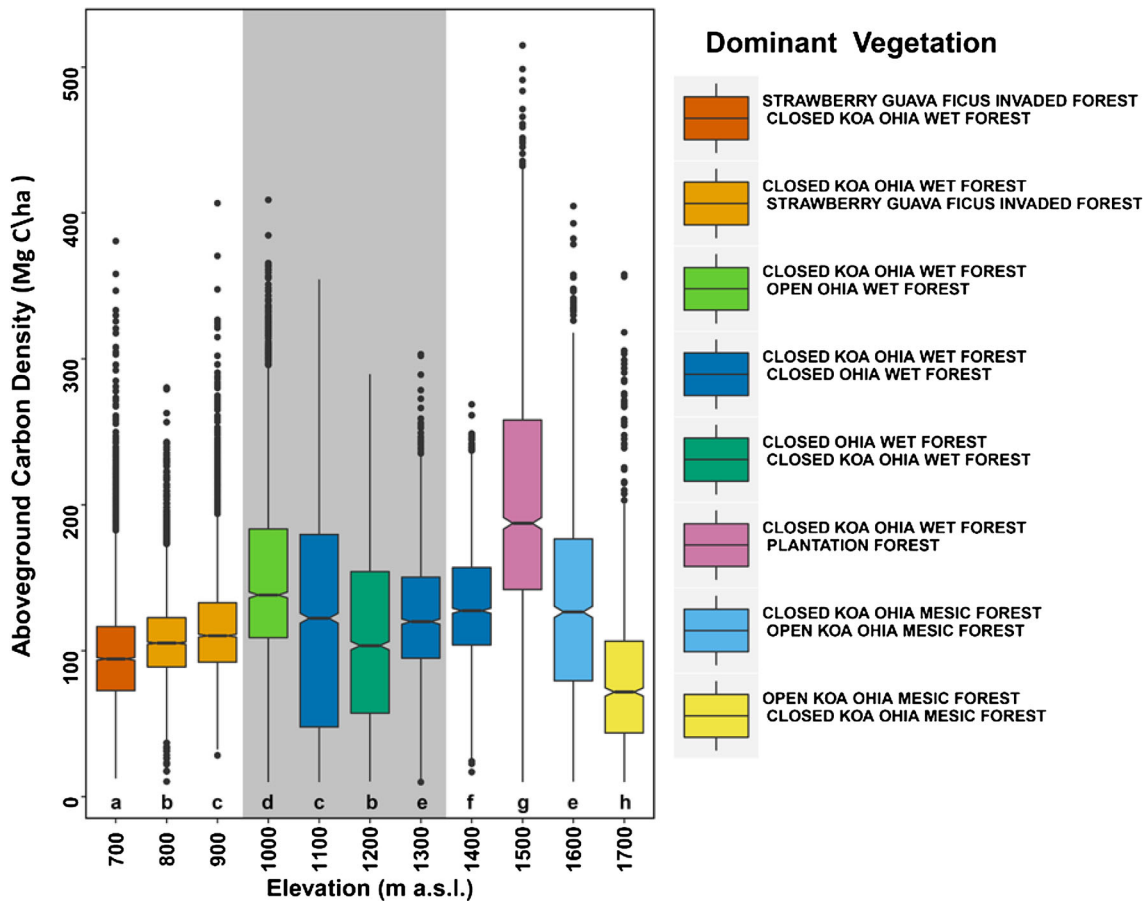


Figure 9. Aboveground carbon density by elevation. Elevations with *different lowercase letters* above the X-axis differ statistically ( $p < 0.05$ ). The boxplots are *color-coded* by the two most dominant forest types at each elevation; see Table 1 for percent cover for all forest types at present at each elevation. The elevations between 1000 and 1300 m shown in *gray* are the least impacted by invasive species (Color figure online).

models. For example, soil type had a greater influence on both foliar N and ACD models and may be mitigating variation that would otherwise be present due to substrate age alone. Additionally, Asner and others (2009) found that, in the high-fertility soils of Laupāhoehoe, aboveground biomass was more closely tied to climate than to substrate age.

Topographic relief at Laupāhoehoe exists as small ridges and valleys (<100 m relief) found throughout the reserve (Figure 3). This differs from a similar study of foliar N in a highly dissected lowland tropical forest, located on the Osa Peninsula, Costa Rica, which found that topography (also <100 m relief) played a stronger role in organizing foliar N (Balzotti and others 2016) and ACD (Taylor and others 2015). Changes in topography at Laupāhoehoe are more subtle, and, when compared to the enormous influence of disturbance, climate, vegetation type, and soil, did not play as

strong a role in influencing spatial patterns of foliar N or ACD. Although topographic variation at the watershed scale contributed little to the overall foliar N and ACD models, coarser topographic scales could have a greater contribution to foliar N and ACD models. For example, Detto and others (2013) showed that, in a Panamanian tropical forest, spatial variation in canopy height was strongly related to topographic curvature measured at scales between 20 and 300 m with a peak correlation at 250 m.

Changes in climate along elevation gradients can result in species turnover and intraspecific leaf morphological and canopy structural changes (Körner and others 1986; Lieberman and others 1996; Cordell and others 1999; Salinas and others 2011). We found that elevation-dependent changes in temperature and precipitation in the study region were associated with foliar N and ACD and thus likely influenced

nutrient cycling rates and soil water content. For example, mass loss and N release during leaf litter decay increase with decreasing elevation and increasing MAT (Bothwell and others 2014). Similarly, on Maui, Schuur and Matson (2001) found that foliar N, soil N availability, and forest growth all decreased with increased precipitation. This pattern of foliar N decrease, coinciding with increased precipitation, was observed despite the overarching humid conditions, where rainfall exceeds plant demand for water (MAP 2000–5000 mm; Schuur and Matson). These conditions were comparable to those found at Laupāhoehoe (MAP 1500–5000 mm). The sharp decrease in ACD with MAP between 3000 and 4000 mm is also similar to Schuur and Matson's (2001) reported declines in annual net primary productivity. The decrease in foliar N and ACD with lower MAT and higher MAP is most likely due to crossing of climate thresholds that can result in a slowing of biological processes, such as decomposition rates.

Much of the observed pattern in canopy N and ACD is the result of individual species responses to available nutrients and climate. Changes to foliar N and ACD, due to non-native vegetation in Laupāhoehoe, are a result of recent anthropogenic land-use changes that began less than 220 years ago, post-European contact. Further invasion into native forests, and or future changes in MAT or MAP, will result in further alteration of biogeochemical cycles and possible changes in ecosystem functioning. With the exception of a few species (for example, tropical ash), shifts away from native forests, in Laupāhoehoe, will likely lead to forests with elevated levels of N and lower ACD (Asner and others 2009, 2016). Although we were unable to validate the remotely sensed foliar N at this time, we know from past studies and ongoing work with a similar sensor configuration and PLSR methodology that the method has consistent precision across tropical forests, with variation in accuracy of only roughly 10%. (Asner and others 2015b; Balzotti and others 2016; Chadwick and Asner 2016; Unpublished data). Future work should focus on whether mid-elevation forests are more resistant to invasive species and their influences, due to existing state factors, such as soil and climate, or whether the phenomenon is merely a result of distance to disturbance. Multi-temporal high-resolution remote sensing will be key to future work in the region, to better understand rates of change and potential resilience and resistance of humid forests.

## ACKNOWLEDGEMENTS

We thank P. Brodrick, C. Anderson, D. Knapp, R. Martin, and N. Vaughn of the Carnegie Airborne Observatory for assistance with data collection and processing, and J. Barbosa for advice. The Carnegie Airborne Observatory has been made possible by grants and donations to G. P. Asner from the Avatar Alliance Foundation, Margaret A. Cargill Foundation, David and Lucile Packard Foundation, Gordon and Betty Moore Foundation, Grantham Foundation for the Protection of the Environment, W. M. Keck Foundation, John D. and Catherine T. MacArthur Foundation, Andrew Mellon Foundation, Mary Anne Nyburg Baker and G. Leonard Baker Jr, and William R. Hearst III.

## REFERENCES

- Allison SD, Vitousek PM. 2004. Rapid nutrient cycling in leaf litter from invasive plants in Hawai'i. *Oecologia* 141:612–19.
- Amundson R, Jenny H. 1991. The place of humans in the state factor theory of ecosystems and their soils. *Soil Sci* 151:99–100.
- Asner G, Elmore A, Hughes R, Warner A, Vitousek PM. 2005. Ecosystem structure along bioclimatic gradients in Hawai'i from imaging spectroscopy. *Remote Sens Environ* 96:497–508.
- Asner GP, Anderson CB, Martin RE, Tupayachi R, Knapp DE, Sinca F. 2015a. Landscape biogeochemistry reflected in shifting distributions of chemical traits in the Amazon forest canopy. *Nat Geosci* 8:567–73.
- Asner GP, Hughes R, Varga TA, Knapp DE, Kennedy-Bowdoin T. 2009. Environmental and biotic controls over aboveground biomass throughout a tropical rain forest. *Ecosystems* 12:261–78.
- Asner GP, Hughes RF, Vitousek PM, Knapp DE, Kennedy-Bowdoin T, Boardman J, Martin RE, Eastwood M, Green RO. 2008. Invasive plants transform the three-dimensional structure of rain forests. *Proc Natl Acad Sci USA* 105:4519–23.
- Asner GP, Knapp DE, Kennedy-Bowdoin T, Jones MO, Martin RE, Boardman J, Field CB. 2007. Carnegie Airborne Observatory: in-flight fusion of hyperspectral imaging and waveform light detection and ranging for three-dimensional studies of ecosystems. *J Appl Remote Sens* 1:13536.
- Asner GP, Martin RE, Anderson CB, Knapp DE. 2015b. Quantifying forest canopy traits: imaging spectroscopy versus field survey. *Remote Sens Environ* 158:15–27.
- Asner GP, Martin RE, Tupayachi R, Anderson CB, Sinca F, Carranza-Jiménez L, Martínez P. 2014. Amazonian functional diversity from forest canopy chemical assembly. *Proc Natl Acad Sci USA* 111:5604–9.
- Asner GP, Sousan S, Knapp DE, Selmants PC, Martin RE, Hughes RF, Giardina CP. 2016. Rapid forest carbon assessments of oceanic islands: a case study of the Hawaiian archipelago. *Carbon Balance Manag* 11:1.
- Ballice RG, Miller JD, Oswald BP, Edminster C, Yool SR. 2000. Forest surveys and wildfire assessment in the Los Alamos region, 1998–1999. Los Alamos Nat. Lab., LA-13714-MS.

- Balzotti CS, Asner GP, Taylor PG, Cleveland CC, Cole R, Martin RE, Nasto M, Osborne BB, Porder S, Townsend AR. 2016. Environmental controls on canopy foliar nitrogen distributions in a Neotropical lowland forest. *Ecol Appl* 26:2451–64.
- Bonan GB. 2008. Forests and climate change: forcings, feedbacks, and the climate benefits of forests. *Science* 320(5882):1444–9.
- Bothwell LD, Selmants PC, Giardina CP, Litton CM. 2014. Leaf litter decomposition rates increase with rising mean annual temperature in Hawaiian tropical montane wet forests. *PeerJ* 2:e685.
- Brady NC, Weil RR. 2000. Elements of the nature and properties of soils. Upper Saddle River (NJ): Prentice Hall.
- Broadbent EN, Zambrano AMA, Asner GP, Field CB, Rosenheim BE, Kennedy-Bowdoin T, Knapp DE, Burke D, Giardina C, Cordell S. 2014. Linking rainforest ecophysiology and microclimate through fusion of airborne LiDAR and hyperspectral imagery. *Ecosphere* 5:1–37.
- de Castilho CV, Magnusson WE, de Araújo RNO, Luizão RCC, Luizão FJ, Lima AP, Higuchi N. 2006. Variation in above-ground tree live biomass in a central Amazonian forest: effects of soil and topography. *For Ecol Manag* 234:85–96.
- Chadwick K, Asner G. 2016. Organismic-scale remote sensing of canopy foliar traits in lowland tropical forests. *Remote Sens* 8:87.
- Chen Y, Han W, Tang L, Tang Z, Fang J. 2013. Leaf nitrogen and phosphorus concentrations of woody plants differ in responses to climate, soil and plant growth form. *Ecography (Cop)* 36:178–84.
- Cleveland CC, Townsend AR, Taylor P, Alvarez-Clare S, Bustamante MMC, Chuyong G, Dobrowski SZ, Grierson P, Harms KE, Houlton BZ, Marklein A, Parton W, Porder S, Reed SC, Sierra CA, Silver WL, Tanner EVJ, Wieder WR. 2011. Relationships among net primary productivity, nutrients and climate in tropical rain forest: a pan-tropical analysis. *Ecol Lett* 14:939–47.
- Colgan MS, Baldeck CA, Féret JB, Asner GP. 2012. Mapping savanna tree species at ecosystem scales using support vector machine classification and BRDF correction on airborne hyperspectral and LiDAR data. *Remote Sens* 4:3462–80.
- Cordell S, Goldstein G, Meinzer FC, Handley LL. 1999. Allocation of nitrogen and carbon in leaves of *Metrosideros polymorpha* regulates carboxylation capacity and  $\delta^{13}C$  along an altitudinal gradient. *Funct Ecol* 13:811–18.
- Craine JM, Elmore AJ, Aidar MPM, Bustamante M, Dawson TE, Hobbie EA, Kahmen A, MacK MC, McLauchlan KK, Michelsen A, Nardoto GB, Pardo LH, Peñuelas J, Reich PB, Schuur EAG, Stock WD, Templer PH, Virginia RA, Welker JM, Wright IJ. 2009. Global patterns of foliar nitrogen isotopes and their relationships with climate, mycorrhizal fungi, foliar nutrient concentrations, and nitrogen availability. *New Phytol* 183:980–92.
- Department of Land and Natural Resources (DNLR), United States Department of Agriculture (USDA). 2016. Laupāhoehoe forest management plan. Honolulu (Hi): Department of Land and Natural Resources, United States Department of Agriculture.
- Detto M, Muller-Landau HC, Mascaro J, Asner GP. 2013. Hydrological networks and associated topographic variation as templates for the spatial organization of tropical forest vegetation. *PLoS ONE* 8:e76296.
- Elith J, Leathwick JR, Hastie T. 2008. A working guide to boosted regression trees. *J Anim Ecol* 77:802–13.
- Evans IS. 1972. General geomorphometry, derivatives of altitude, and descriptive statistics. In: Chorley RJ, Ed. *Spatial analysis in geomorphology*. London: Methuen. p 36.
- Evans JS, Oakleaf J, Cushman SA, Theobald D. 2014. An ArcGIS toolbox for surface gradient and geomorphometric modeling, version 2.0-0. <http://evansmurphy.wix.com/evansspatial>.
- Feilhauer H, Asner GP, Martin RE, Schmidlein S. 2010. Brightness-normalized partial least squares regression for hyperspectral data. *J Quant Spectrosc Radiat Transf* 111:1947–57.
- Field C. 1983. Allocating leaf nitrogen for the maximization of carbon gain: leaf age as a control on the allocation program. *Oecologia* 56:341–7.
- Field C, Mooney HA. 1983. Leaf age and seasonal effects on light, water, and nitrogen use efficiency in a California shrub. *Oecologia* 56:348–55.
- Friedman J. 2001. Greedy function approximation: a gradient boosting machine. *Ann Stat* 29:1189–232.
- Friedman JH, Meulman JJ. 2003. Multiple additive regression trees with application in epidemiology. *Stat Med* 22:1365–81.
- Fyllas NM, Patiño S, Baker TR, Bielefeld Nardoto G, Martinelli LA, Quesada CA, Paiva R, Schwarz M, Horna V, Mercado LM, Santos A, Arroyo L, Jiménez EM, Luizão FJ, Neill DA, Silva N, Prieto A, Rudas A, Silviera M, Vieira ICG, Lopez-Gonzalez G, Malhi Y, Phillips OL, Lloyd J. 2009. Basin-wide variations in foliar properties of Amazonian forest: phylogeny, soils and climate. *Biogeosci Discuss* 6:3707–69.
- Gessler PE, Moore ID, McKenzie NJ, Ryan PJ. 1995. Soil-landscape modelling and spatial prediction of soil attributes. *Int J Geogr Inf Sci* 9:421–32.
- Giambelluca TW, Chen Q, Frazier AG, Price JP, Chen Y-L, Chu P-S, Eischeid JK, Delparte DM. 2013. Online rainfall atlas of Hawai'i. *Bull Am Meteorol Soc* 94:313–16.
- Giambelluca TW, Shuai X, Barnes R, Alliss R, Longman R, Miura T, Chen Q, Frazier A, Mudd R, Cuo L, Businger A. 2014. Final report submitted to the US Army Corps of Engineers—Honolulu District, and the Commission on Water Resource Management, State of Hawai'i.
- Gon SM, Allison A, Cannarella RJ, Jacobi JD, Kaneshiro KY, Kido MH, Lane-Kamahele M, Miller DSE. 2006. A GAP analysis of Hawaii: final report. US Department of the Interior. Washington, DC: US Geological Survey.
- Haaland DM, Thomas EV. 1988. Partial least-squares methods for spectral analyses. 1. Relation to other quantitative calibration methods and the extraction of qualitative information. *Anal Chem* 60:1193–202.
- Hastie T, Tibshirani R, Friedman J. 2009. The elements of statistical learning. *Elements* 1:337–87.
- Hijmans RJ, Phillips S, Leathewick J, Elith J. 2016. Package 'dismo'. Species distribution modeling. R package version 1.0–15.
- Horn BKP. 1981. Hill shading and the reflectance map. *Proc IEEE* 69:14–47.
- Houlton BZ, Morford SL. 2015. A new synthesis for terrestrial nitrogen inputs. *Soil* 1:381–97.
- Hughes RF, Denslow JS. 2005. Invasion by a N<sub>2</sub>-fixing tree alters function and structure in wet lowland forests of Hawaii. *Ecol Appl* 15:1615–28.
- Jenny H. 1941. Factors of soil formation. *Soil Sci* 52:415.
- Kellner J, Asner G. 2009. Convergent structural responses of tropical forests to diverse disturbance regimes. *Ecol Lett* 12(9):887–97.

- Van Kleunen M, Weber E, Fischer M. 2010. A meta-analysis of trait differences between invasive and non-invasive plant species. *Ecol Lett* 13:235–45.
- Körner C, Bannister P, Mark AF. 1986. Altitudinal variation in stomatal conductance, nitrogen content and leaf anatomy in different plant life forms in New Zealand. *Oecologia* 69:577–88.
- Lepine LC, Ollinger SV, Ouimette AP, Martin ME. 2016. Examining spectral reflectance features related to foliar nitrogen in forests: implications for broad-scale nitrogen mapping. *Remote Sens Environ* 173:174–86.
- Levine NM, Zhang K, Longo M, Baccini A, Phillips OL, Lewis SL, Alvarez-Dávila E, Segalin de Andrade AC, Brienen RJW, Erwin TL, Feldpausch TR, Monteagudo Mendoza AL, Nuñez Vargas P, Prieto A, Silva-Espejo JE, Malhi Y, Moorcroft PR. 2016. Ecosystem heterogeneity determines the ecological resilience of the Amazon to climate change. *Proc Natl Acad Sci* 113:793–7.
- Liao C, Peng R, Luo Y, Zhou X, Wu X, Fang C, Chen J, Li B. 2008. Altered ecosystem carbon and nitrogen cycles by plant invasion: a meta-analysis. *New Phytol* 177:706–14.
- Lieberman D, Lieberman M, Peralta R, Hartshorn GS. 1996. Tropical forest structure and composition on a large-scale altitudinal gradient in Costa Rica. *J Ecol* 84:137–52.
- Liu Y, Yu G, Wang Q, Zhang Y. 2014. How temperature, precipitation and stand age control the biomass carbon density of global mature forests. *Glob Ecol Biogeogr* 23:323–33.
- Luizão RCC, Luizão FJ, Paiva RQ, Monteiro TF, Sousa LS, Kruijt B. 2004. Variation of carbon and nitrogen cycling processes along a topographic gradient in a central Amazonian forest. *Glob Change Biol* 10:592–600.
- McCune B, Keon D. 2002. Equations for potential annual direct incident radiation and heat load. *J Veg Sci* 13:603–6.
- McNeil BE, Read JM, Driscoll CT. 2012. Foliar nitrogen responses to the environmental gradient matrix of the Adirondack Park, New York. *Ann Assoc Am Geogr* 102:1–16.
- McNeil BE, Read JM, Sullivan TJ, McDonnell TC, Fernandez JJ, Driscoll CT. 2008. The spatial pattern of nitrogen cycling in the Adirondack Park, New York. *Ecol Appl* 18:438–52.
- Moisen GG, Freeman EA, Blackard JA, Frescino TS, Zimmermann NE, Edwards TC. 2006. Predicting tree species presence and basal area in Utah: a comparison of stochastic gradient boosting, generalized additive models, and tree-based methods. *Ecol Model* 199:176–87.
- Moore I, Gessler P, Nielsen GA, Peterson GA. 1993. Soil attribute prediction using terrain analysis. *Soil Sci Soc Am J* 57:443–52.
- Morris RJ. 2010. Anthropogenic impacts on tropical forest biodiversity: a network structure and ecosystem functioning perspective. *Philos Trans R Soc B Biol Sci* 365:3709–18.
- Ollinger SV, Smith ML, Martin ME, Hallett RA, Goodale CL, Aber JD. 2002. Regional variation in foliar chemistry and N cycling among forests of diverse history and composition. *Ecology* 83:339–55.
- Pickett ST. 1989. Space-for-time substitution as an alternative to long-term studies. In: *Long-term studies in ecology*. New York: Springer. pp 110–35.
- Pike RJ, Wilson SE. 1971. Elevation-relief ratio, hypsometric integral, and geomorphic area-altitude analysis. *Geol Soc Am Bull* 82:1079.
- Porder S. 2015. Linking geomorphology, weathering and cation availability in the Luquillo Mountains of Puerto Rico. *Geoderma* 249–250:100–10.
- Quesada CA, Phillips OL, Schwarz M, Czimczik CI, Baker TR, Patiño S, Fyllas NM, Hodnett MG, Herrera R, Almeida S, Alvarez-Dávila E, Arneeth A, Arroyo L, Chao KJ, Dezzio N, Erwin T, di Fiore A, Higuchi N, Honorio Coronado E, Jimenez EM, Killeen T, Lezama AT, Lloyd G, López-González G, Luizão FJ, Malhi Y, Monteagudo A, Neill DA, Núñez Vargas P, Paiva R, Peacock J, Peñuela MC, Peña Cruz A, Pitman N, Priante Filho N, Prieto A, Ramírez H, Rudas A, Salomão R, Santos AJB, Schmerler J, Silva N, Silveira M, Vásquez R, Vieira I, Terborgh J, Lloyd J. 2012. Basin-wide variations in Amazon forest structure and function are mediated by both soils and climate. *Biogeosciences* 9:2203–46.
- R Development Core Team R. 2016. R: a language and environment for statistical computing. R Found Stat Comput Austria. <https://www.R-project.org/>.
- Rien A, Chapin FS. 2000. The mineral nutrition of wild plants revisited: a re-evaluation of processes and patterns. *Adv Ecol Res* 30:1–67.
- Sakai AK, Wagner WL, Mehrhoff LA. 2002. Patterns of endangerment in the Hawaiian Flora. *Syst Biol* 51:276–302.
- Salinas N, Malhi Y, Meir P, Silman M, Roman Cuesta R, Huaman J, Salinas D, Huaman V, Gibaja A, Mamani M, Farfan F. 2011. The sensitivity of tropical leaf litter decomposition to temperature: results from a large-scale leaf translocation experiment along an elevation gradient in Peruvian forests. *New Phytol* 189:967–77.
- Sappington JM, Longshore KM, Thompson DB. 2007. Quantifying landscape ruggedness for animal habitat analysis: a case study using bighorn sheep in the Mojave Desert. *J Wildl Manag* 71:1419–26.
- Schuur EA, Matson PA. 2001. Net primary productivity and nutrient cycling across a mesic to wet precipitation gradient in Hawaiian montane forest. *Oecologia* 128:431–42.
- Selmants PC, Giardina CP, Jacobi JD, Zhu Z. 2017. Baseline and projected future carbon storage and carbon fluxes in ecosystems of Hawai'i. US Geological Survey Professional Paper 1834.
- Selmants PC, Litton CM, Giardina CP, Asner GP. 2014. Ecosystem carbon storage does not vary with mean annual temperature in Hawaiian tropical montane wet forests. *Glob Change Biol* 20:2927–37.
- Sherrod D, Sinton J, Watkins S. 2007. Geologic map of the State of Hawai'i. US Geological Survey.
- Singh A, Serbin SP, McNeil BE, Kingdon CC, Townsend PA. 2015. Imaging spectroscopy algorithms for mapping canopy foliar chemical and morphological traits and their uncertainties. *Ecol Appl* 25:2180–97.
- Stage AR. 1976. An expression for the effect of aspect, slope, and habitat type on tree growth note by A. R. Stage. *For Sci* 22:457–60.
- Taylor P, Asner G, Dahlin K, Anderson C, Knapp D, Martin R, Mascaro J, Chazdon R, Cole R, Wanek W, Hofhansl F, Malavassi E, Vilchez-Alvarado B, Townsend A. 2015. Landscape-scale controls on aboveground forest carbon stocks on the Osa Peninsula, Costa Rica. *PLoS ONE* 10:e0126748.
- Tickitt T, Whitehead AN, Fraiola H. 2006. Traditional gathering of native hula plants in alien-invaded Hawaiian forests: adaptive practices, impacts on alien invasive species and conservation implications. *Environ Conserv* 33:185.
- Townsend AR, Vitousek PM, Trumbore SE. 1995. Soil organic matter dynamics along gradients in temperature and land use on the island of Hawaii. *Ecology* 76:721–33.

- Townsend PA, Foster JR, Chastian RA Jr, Currie WS. 2003. Canopy nitrogen in the forests of the Central Appalachian Mountains using Hyperion and AVIRIS. *IEEE Trans Geosci Remote Sens* 41:1347–54.
- Vilà M, Espinar JL, Hejda M, Hulme PE, Jarošík V, Maron JL, Pergl J, Schaffner U, Sun Y, Pyšek P. 2011. Ecological impacts of invasive alien plants: a meta-analysis of their effects on species, communities and ecosystems. *Ecol Lett* 14:702–8.
- Vitousek P. 2004. Nutrient cycling and limitation Hawaii as a model system. Princeton: Princeton University Press.
- Vitousek PM, Aplet G, Turner D, Lockwood JJ. 1992. The Mauna Loa environmental matrix: foliar and soil nutrients. *Oecologia* 89:372–82.
- Vitousek PM, Farrington H. 1997. Nutrient limitation and soil development: experimental test of a biogeochemical theory. *Biogeochemistry* 37:63–75.
- Vitousek PM, Field CB, Matson PA. 1990. Variation in foliar  $\delta^{13}\text{C}$  in Hawaiian *Metrosideros polymorpha*: a case of internal resistance? *Oecologia* 84:362–70.
- Vitousek PM, Jerry M. 1979. Nitrate patterns losses from disturbed forests: pattern and mechanisms. *Society* 25:605–19.
- Vitousek PM, Turner DR, Kitayama K. 1995. Foliar nutrients during long-term soil development in Hawaiian montane rain forest. *Ecology* 76:712–20.
- Woodward FI, Smith TM, Emanuel WR. 1995. A global land primary productivity and phytogeography model. *Glob Biogeochem Cycles* 9:471–90.
- Wright DJ, Pendleton M, Boulware J, Walbridge S, Gerlt B, Eslinger D, Sampson D, Huntley E. 2012. ArcGIS Benthic Terrain Modeler (BTM), v. 3.0, Environmental Systems Research Institute, NOAA Coastal Services Center, Massachusetts Office of Coastal Zone Management. <http://esriurl.com/5754>.
- Zevenbergen LW, Thorne CR. 1987. Quantitative analysis of land surface topography. *Earth Surf Process Landf* 12:47–56.
- Zolkos SG, Goetz SJ, Dubayah R. 2013. A meta-analysis of terrestrial aboveground biomass estimation using lidar remote sensing. *Remote Sens Environ* 128:289–98.